NEUROSCIENCE of Consciousness

Neuroscience of Consciousness, 2024, **2024(1)**, niae027

DOI: https://doi.org/10.1093/nc/niae027

Research Article

Content–state dimensions characterize different types of neuronal markers of consciousness

Pauline Pérez[1,2,3,†], Dragana Manasova[1,4,†], Bertrand Hermann[1,4,5], Federico Raimondo[1,6,7], Benjamin Rohaut[1,3], Tristán A. Bekinschtein[8], Lionel Naccache[1,9], Anat Arzi[1,8,10], Jacobo D. Sitt[1,*]

[1]Institut du Cerveau - Paris Brain Institute, Inserm, CNRS, Sorbonne Université, Paris 75013, France
[2]Hospice Civils de Lyon—HCL, Département anesthésie-réanimation, Hôpital Edouard Herriot
[3]Neuro ICU, DMU Neurosciences, AP-HP, Hôpital de la Pitié Salpêtrière, Paris 75013, France
[4]Université Paris Cité, Paris 75006, France
[5]Medical Intensive Care Unit, HEGP Hôpital, Assistance Publique—Hôpitaux de Paris-Centre (APHP-Centre), Paris 75015, France
[6]Institute of Neuroscience and Medicine (INM-7: Brain and Behaviour), Research Centre Jülich, Jülich 52428, Germany
[7]Institute of Systems Neuroscience, Heinrich Heine University Düsseldorf, Dusseldorf 40225, Germany
[8]Consciousness and Cognition Lab, Department of Psychology, University of Cambridge, Cambridge CB2 3EB, United Kingdom
[9]AP-HP, Hôpital Pitié-Salpêtrière, Service de Neurophysiologie Clinique, Paris 75013, France
[10]Department of Medical Neurobiology, Institute for Medical Research Israel Canada and Department of Cognitive and Brain Sciences, Hebrew University of Jerusalem, Jerusalem, Israel

[†]Co-first authors.
*Corresponding author. Department of Cognitive and Brain Sciences, Institut du Cerveau—Paris Brain Institute—ICM, Inserm, CNRS, Sorbonne Université, Paris 75013, France.
E-mail: jacobo.sitt@icm-institute.org

Abstract

Identifying the neuronal markers of consciousness is key to supporting the different scientific theories of consciousness. Neuronal markers of consciousness can be defined to reflect either the brain signatures underlying specific conscious content or those supporting different states of consciousness, two aspects traditionally studied separately. In this paper, we introduce a framework to characterize markers according to their dynamics in both the "state" and "content" dimensions. The 2D space is defined by the marker's capacity to distinguish the conscious states from non-conscious states (on the *x*-axis) and the content (e.g. perceived versus unperceived or different levels of cognitive processing on the *y*-axis). According to the sign of the *x*- and *y*-axis, markers are separated into four quadrants in terms of how they distinguish the state and content dimensions. We implement the framework using three types of electroencephalography markers: markers of connectivity, markers of complexity, and spectral summaries. The neuronal markers of state are represented by the level of consciousness in (i) healthy participants during a nap and (ii) patients with disorders of consciousness. On the other hand, the neuronal markers of content are represented by (i) the conscious content in healthy participants' perception task using a visual awareness paradigm and (ii) conscious processing of hierarchical regularities using an auditory local–global paradigm. In both cases, we see separate clusters of markers with correlated and anticorrelated dynamics, shedding light on the complex relationship between the state and content of consciousness and emphasizing the importance of considering them simultaneously. This work presents an innovative framework for studying consciousness by examining neuronal markers in a 2D space, providing a valuable resource for future research, with potential applications using diverse experimental paradigms, neural recording techniques, and modeling investigations.

Keywords: consciousness; sleep; conscious content; disorders of consciousness; neuronal markers of consciousness

Introduction

Giving a definition of consciousness with a coherent theoretical framework is a daunting task that would benefit from simple conceptual dissociations to improve interpretability. Identifying the neural correlates of consciousness has become crucial to allow progress in the science of consciousness. Following the Koch and Crick seminal definition, neural correlates of consciousness are the minimal neural processes that must occur in the brain for a particular conscious experience to occur (Crick and Koch 1990). However, this definition leaves the possibility of multiple types of neuronal markers of consciousness, two of which are those of conscious contents and those of states of consciousness.

Traditionally, research on consciousness has developed separately in these two pillars. While some researchers, mainly

Received 8 November 2023; revised 30 May 2024; accepted 8 June 2024

cognitive neuroscientists, primarily focused on the neuronal processes behind conscious access of specific content (e.g. the capacity to report stimuli as seen versus not seen or to discriminate stimuli). The second line of researchers focused on global states of consciousness (e.g. sleep, anesthesia, and disorders of consciousness) (Goupil and Bekinschtein 2012, Sanders et al. 2012, Boly et al. 2013, Bayne et al. 2016). This research has been rather developed by physicians with questions of diagnosis and prognosis often sanctioned by ethical and end-of-life questions.

Neuronal markers of content (NM-Cs) are a reflection of the neural processes that occur for a specific experience. On one hand, NM-Cs are studied by comparing conditions where specific conscious content (e.g. perception of sound or image) is present or absent while stimulus properties and the state of consciousness remain unchanged. The difference between the neural activities averaged by trials depending on the capacity to report (reported perceived, e.g. "seen") compared to the lack of capacity to report (reported not perceived, e.g. "unseen") is generally considered to be a marker of access content. Several different paradigms exist such as perceptual suppression, masking, or threshold paradigms in different sensory modalities (Kim and Blake 2005, Del Cul et al. 2007, Dehaene and Changeux 2011). On another hand, there are tasks that assess the capacity to attend and integrate perceptual and cognitive hierarchical regularities such as the auditory local–global (LG) paradigm (Bekinschtein et al. 2009). The two different types of paradigms and examples show a gradient of content—where one end is about the mentioned access consciousness (seen/unseen), and on the other hand is the processing of hierarchical regularities (the LG paradigm as an example). Various methods such as electroencephalography (EEG), magnetoencephalography, or functional magnetic resonance imaging (fMRI) allow for studying the neural correlates of these conscious perceptual experiences (Tsuchiya et al. 2015, Koch et al. 2016). From these studies, the NM-Cs differentiate the "seen" from the "unseen" range from the primary and secondary networks of early perceptual and cognitive integration to abstract cognitive implementation associative areas (Dehaene and Changeux 2011). Electrophysiological studies on monkeys and humans have revealed several signatures of auditory awareness like P3b event-related potentials and oscillations in α/β (9–30 Hz) and γ (>40 Hz) bands between the visual cortex and frontoparietal cortices (Dehaene and Changeux 2011).

Neuronal markers of state (NM-Ss) are used to differentiate states of consciousness. These include conditions as diverse as sleep, partial complex seizures, general anesthesia, and patients in an unresponsive wakefulness syndrome (UWS) or minimally consciousness state (Laureys et al. 2004). NM-Ss can signal the emergence of consciousness, with the brain having to be at an appropriate level of processing to "ensure adequate cortical excitability" for the emergence of consciousness (Koch et al. 2016). Consciousness disorders in patients with brain injury are a good model as they provide a spectrum of different conscious states. The current taxonomy to describe these patients is based on behavioral responsiveness [Coma Recovery Scale-Revised, CRS-R (Kalmar and Giacino 2005)]. This evaluation classifies these patients in different clinical conditions: UWS (Laureys et al. 2010)—previously called the vegetative state, characterized by a behavioral examination of preserved reflexive behavior, such as eye-opening and spontaneous breathing, without apparent awareness of self and the environment (Jennett and Plum 1972). The second clinical condition is the minimally conscious state (MCS) [more recently proposed to be renamed as cortically mediated state (Naccache 2018)], where patients show reproducible behavioral responses, suggesting environmental awareness, such as slow visual pursuit or response to simple commands; and finally, the emergence from MCS, where the patient is able to maintain some degree of basic communication (Giacino et al. 2002). These three clinical categories can be considered "ordered" in a gradient reflecting the richness of conscious experience (Bayne et al. 2016). Additionally, MCS can be subcategorized into MCS– and MCS+. MCS– refers to patients who demonstrate non-reflexive behaviors like visual pursuit and orientation to stimuli, whereas MCS+ denotes patients capable of more advanced behaviors such as command following and verbalization, signifying higher levels of awareness and communication ability within the MCS spectrum (Bruno et al. 2011, Edlow et al. 2021) (for a review, see Edlow et al. (2021) on further details of disorders of consciousness (DoC) and the patients' emergence).

The theoretical and behavioral findings are also verified—and in many cases enriched (Naccache 2018)—by NM-Ss. For example, different electrophysiological markers derived from EEG recording in a resting state (Chennu et al. 2014, Sitt et al. 2014) are able to discriminate UWS patients from MCS patients. In the same way, fMRI during a resting state period (Demertzi et al. 2014, 2015, 2019, Di Perri et al. 2016), positron emission tomography with metabolic markers (Stender et al. 2014, Hermann et al. 2021b) or the calculation of an index reflecting the EEG reaction after stimulation by transcranial magnetic stimulation (Casarotto et al. 2016), is capable of discriminating between UWS and MCS patients. This contrast makes it possible to study the UWS as a state of wakefulness without awareness, and the MCS as a state with minimal behaviors consistent with awareness of the environment or the self. Sleep provides an additional valuable model of altered and reversible states of consciousness, with the advantage of the possibility of recording NM-Ss in healthy participants. Indeed, there are clear EEG markers (Comsa et al. 2019, Imperatori et al. 2021, Manasova and Stankovski 2023) and fMRI activity patterns characterizing brain activity in wakefulness and during different sleep stages (Dang-Vu et al. 2010, Peigneux 2014, Song and Tagliazucchi 2020). Additional models of interest include anesthesia (Lewis et al. 2012, Barttfeld et al. 2015, Chennu et al. 2016, Zelmann et al. 2023) or complex seizures (Guo et al. 2016, Blumenfeld 2021).

Hence, there is rich literature studying particular brain activity features as putative NM-Ss or NM-Cs. However, not much is known when it comes to comparing those given features on both dimensions simultaneously. While several studies have attempted to study content and state separately, a theoretical development proposes a 3D axis with an x-axis corresponding to subjective conscious content (as reported by the participant), the y-axis to the objective state of consciousness (defined by behavior and body signals), and the z-axis to a subjective state of consciousness (as reported by the participant) (Bachmann 2012). In the examples presented here, we used markers of objective state of consciousness in the y-axis. However, the proposed framework is also compatible when subjective state markers are considered. Bayne and colleagues, on the other hand, propose a multidimensional graph like a radar chart with different axes (Bayne et al. 2016): content-related (e.g. content gating and content range) and functional dimensions (e.g. relating to attentional control, memory consolidation, verbal report, reasoning, and action selection). The problem with this representation is that it is difficult to standardize and, hence, less applicable. Interestingly, Sergent et al. (2017) created a unique EEG protocol allowing the exploration of eight axes (own name recognition, temporal attention, spatial attention, detection of spatial incongruence motor planning, and

modulations of these effects by the global context) but the construction of such a paradigm is complex. For Chalmers, studying content and conscious state at the same time is difficult in experimental conditions (Chalmers 1997), with most studies contrasting variable content in a given state of consciousness or studying brain differences in different states.

A pertinent perspective to note is that the categorization of state and content is nuanced. Recent work shows that these categories are part of a spectrum that often overlaps (Andrillon 2023, Andrillon and Oudiette 2023). On one hand, we have sensory processing during different levels of arousal (Andrillon and Kouider 2020); content during states of low arousal (Solms 2000, Leslie et al. 2007); responsiveness to the environment during lucid dreams and other sleep stages (Türker et al. 2023); and phenomena such as mind-wandering and mind-blanking during active wakefulness, which are hypothesized to originate from local sleep occurrences (Andrillon et al. 2021). However, in all of these cases, the content and state dimensions are present and can be disentangled using subjective and objective measures (albeit without an existing unit of measurement and based on assumptions, which should always be well reported).

The simultaneous study of state and content neural correlates implies the following research question: what is the relationship of different neuronal markers in a 2D space of level and content of consciousness axes? Importantly, the same neuronal marker (e.g. delta power) can either reflect the same or different neuronal process across levels and contents of consciousness. To address this question, we introduce a simple framework comprising a 2D space to examine brain features across both dimensions concurrently. This approach facilitates the characterization of various types of markers based on their positioning within the 2D space. We explore this space using two experimental examples: a comparison of states of consciousness (normal sleep or disorders of consciousness) and types of conscious content (auditory or visual). In this 2D space, we put the directionality of different EEG markers when contrasting two conditions (e.g., perceived versus not-perceived or different levels of cognitive processing in the case of the content exploration; and a global state of consciousness versus a global state of unconsciousness in the case of the state exploration). The capacity of the markers to distinguish the contrasted conditions is measured using an Area Under the receiver operating characteristic (ROC) Curve (AUC). The framework's capability to assess simply the behavior of neuronal markers on the state and content conditions demonstrates its relevance to the consciousness research community.

Materials and methods

In this study, we included three separate cohorts of healthy controls and one patient population with disorders of consciousness. Each of the separate groups of healthy controls came in for one of the following EEG experiments: the visual masking paradigm (Del Cul et al. 2007), a session consisting of a period of resting wakefulness followed by a nap, and an experiment using the LG paradigm (Bekinschtein et al. 2009). Whereas the patient population underwent EEG recordings during the LG paradigm (Bekinschtein et al. 2009).

Population

Healthy participants

Healthy participants were recruited on three separate occasions for three distinct experimental paradigms. The inclusion criteria were normal hearing, normal or corrected vision, and no history of neurological, psychiatric, or sleep disorder.

For the first experiment, using the visual awareness paradigm, which took place in Paris, France, we recruited 35 participants (28 women; age = 24.9 ± 4.1 years). For the second experiment, which took place in Cambridge, UK, participants came to the lab to be recorded during wakefulness and a nap period. In this study, 26 participants (19 women; age = 24.3 ± 4.9 years) were recruited and gave written informed consent to procedures approved by the University of Cambridge Research Ethics Committee, in accordance with the Declaration of Helsinki. For the third experiment, we recorded 36 participants (29 women; age = 25.3 ± 3.8 years) for the LG paradigm. The first and the third experiments which took place in Paris, France, were approved by the Ethical Committee of the Pitie Salpetriere Hospital, NeuroDoc protocol. In conformation to the protocol, participants gave written consent before the experiments took place.

Patients

We screened 443 patients (177 women; age = 47.2 ± 19.4 years) recorded between 2008 and 2019 in the neuro-intensive care at Pitié Salpetrière for an expert assessment of their consciousness. During this evaluation, we performed several exams (clinical assessment, magnetic resonance imaging, EEG, event-related potentials, positron emission tomography) to determine more accurately the state of consciousness. In the study, we included only patients assessed to be either in a UWS or MCS according to the best CRS-R score out of five completed during the evaluation week. Out of all the screened patients, we included 388 patients, who, according to the CRS-R behavioral exam, were in an MCS ($N = 191$) or in a UWS ($N = 197$). The patients were in a disorder of consciousness resulting from various etiologies either traumatic or non-traumatic. Because patients were non-communicating, informed consents were obtained from the patient's relatives. The ethical committee of the Pitie-Salpetriere Hospital approved this research under the French label of "routine care research" (Comité de Protection des Personnes no. 2013-A01385-40 Ile de France, Paris, France, under the code "Recherche en soins courants").

Paradigms

Experiment 1: visual awareness paradigm

The first group of healthy controls ($N = 35$, recorded in Paris) underwent EEG recordings of the visual awareness paradigm. Near-threshold visual awareness was assessed using a visual backward masking paradigm modified from Del Cul et al. (2007). This visual awareness paradigm is designed to suppress visual perception by presenting a visual stimulus ("mask") immediately after another visual stimulus ("target"). This manipulation causes a perception failure of the first stimulus. In this paradigm, a para-foveal numerical target ("2", "3", "7", or "8", height = 1.7 cm, width = 1.1 cm) was presented for 16 ms either to the right or to the left of a central fixation point (8° visual angle) on a 60-Hz frame rate screen. The numerical target was followed after a variable Stimulus Onset Asynchrony (SOA, to 16 ms at 83 ms) by a visual mask, consisting of letters surrounding the target, presented for 250 ms. After the target presentation at 800 ms, participants were asked to perform a subjective task of visibility rating of the target through a binary "seen"/"unseen" answer. Answers were collected via key press with a pseudo-randomization of response hand order and switch of response hand in the middle of the task. The entire task consisted of the presentation of 400 trials (64 trials per SOA

and 80 catch trials in which only a mask was presented, without a target).

Experiment 2: nap

The second group of healthy controls ($N = 26$, recorded in Cambridge) underwent EEG recordings during a nap. Participants arrived at the EEG lab either at 8:00 or at 13:00 and were accommodated in a bed and instructed that they have a 2-h window during which they could fall asleep. They were informed that, while asleep, they might be presented with tones via the headphones and that, if they noticed them, they could ignore them and continue sleeping. The EEG signal was constantly monitored for markers of sleep. After having assessed stable non-rapid eye movement (NREM) Stage 2 sleep for at least 3 min, auditory stimulation including pure tones (500–5302 Hz, 100 ms, inter-stimulus interval = 500 ms) was started. Tones were played with a slow fading-in to minimize the likelihood that participants would be awakened by the onset of the stimuli. Importantly, to minimize exposure to stimulation during arousals, whenever arousal occurred stimulation was promptly stopped. Stimulation would then be resumed only after a stable NREM sleep had been reassessed. For the goal of this study, we used sections of the recording during which no sounds were presented.

Experiment 3: LG paradigm

The LG task is an oddball auditory paradigm that has two hierarchical levels of regularities: a "local" regularity that triggers early responses that are preserved in conscious and unconscious states, and a "global" regularity that triggers late evoked responses that are only present in awake, conscious, and attentive participants (Bekinschtein et al. 2009, Wacongne et al. 2011, Chennu et al. 2013, King et al. 2013, Strauss et al. 2015). The neural responses to the violation of each of these regularities can be quantified from two complementary contrasts: the local contrast [local deviant (LD) trials versus local standard (LS) trials] and the global contrast [global deviant (GD) trials versus global standard (GS) trials]. The LG paradigm is developed by Bekinschtein et al. (2009), and it is based on the repetition of two sequences of tones: XXXXX or XXXXY. In a low level (local regularity), XXXXX is the LS and XXXXY is the LD. The contrast between these two sequences reveals the occurrence of the mismatch negativity. This response is in a short range and is also reproduced during the loss of consciousness associated with sleep, general anesthesia, or UWS. In a high level (global regularities), the repetition of the XXXXY or XXXXX is the standard condition and establishes the rule. In this case, we distinguish a GS rule and a GD. The violation of this regularity by the other sequence: XXXXX or XXXXY, respectively, is represented by the P3b waveform and requires conscious awareness and working memory (Bekinschtein et al. 2009) [although see Sergent et al. (2021) for an updated view of P300]. Local and global regularities are manipulated orthogonally 2×2: the first type of blocks consists of LS–GS (XXXXX) and LD–GD (XXXXY) sounds. The second type of blocks is made up of LD–GS (XXXXY) and LS–GD (XXXXX) sounds. Both the patient cohort and the first group of healthy controls ($N = 36$, recorded in Paris) underwent EEG recordings of the LG paradigm. However, in the patient group, we computed the markers from segments of "pseudo-resting-state" [during the first four repeated auditory stimuli (Engemann et al. 2018)] to contrast their power to index the different states of consciousness in patients regardless of the stimulus content (Sitt et al. 2014).

EEG data processing

Experiment 1: visual awareness paradigm

High-density scalp EEG was acquired using 256 electrodes Hydrocel Geodesic Sensor Net on a Net300 Amplifier (Electrical Geodesics Inc. system) with a sampling frequency of 250 Hz during the behavioral task. Impedances were set to <75 kΩ before the start of each recording. Electrodes with voltages >100 μV in more than 50% of the epochs were removed. Moreover, voltage variance was computed across all correct electrodes. Electrodes with a voltage variance Z-score of >4 were removed. This process was repeated four times. Bad electrodes were interpolated using a spline method (Perrin et al. 1989). Epochs were labeled as bad and discarded when voltage exceeded 100 μV in >10% of electrodes. Moreover, voltage variance was computed across all correct epochs, and epochs with a Z-score of >4 were removed. This process was also repeated four times. Average reference was applied to the remaining epochs. Preprocessing was implemented using the MNE-Python package. To get rid of the confound of evoked responses to the mask, we proceeded to a mask subtraction procedure as in the study by Del Cul et al. (2007). We first realigned all epochs to the mask onset and computed the evoked response to the mask from the catch trials. We then subtracted this evoked response from all other trials. Finally, we realigned epochs on the target to obtain epochs stripped from the mask response (this procedure resulted in shortening the epochs which as a result went from −232 to 732 ms after target onset). The window of interest is between the presentation of the numerical target (0 ms) and +700 ms.

Experiment 2: nap

The EEG signal was recorded with 128-channel sensors using a GES 300 Electrical Geodesic amplifier, at a sampling rate of 500 Hz (Electrical Geodesics Inc. system/Philip Neuro). Conductive gel was applied to each electrode to ensure that the impedance between the scalp and electrodes was kept <70 kΩ.

Two independent and experienced sleep examiners blind to stimuli onset/offset times scored offline 30 s-long windows of EEG data according to established guidelines (Berry et al. 2012). The two scoring lists were subsequently compared and controversial epochs were inspected again and discussed until an agreement was reached. EEG and EOG signals were first re-referenced to mastoids and then EEG signals were band-pass filtered between 0.1 and 45 Hz, EOG between 0.2 and 5 Hz. EEG signals were obtained from local derivation and were high-pass filtered >20 Hz. Then, based on the sleep scoring, periods of wakefulness (319.4 ± 33.5 s) and NREM Stage 2 sleep (369.8 ± 93.6 s) when no auditory stimulation was presented were selected. The nap EEG data was split into epochs of 800 ms, separately for the periods of NREM Stage 2 sleep or wakefulness. The epoching was done using a random jitter, between two epochs, from 550 to 850 ms. The EEG recordings were then preprocessed using the same fully automatic procedure as for the visual awareness and the LG paradigms.

Experiment 3: LG paradigm

The EEG data were recorded at a sampling frequency of 250 Hz with a 256-electrode Geodesic Sensor Net (Electrical Geodesic Inc. system) referenced to the vertex. Trials were band-pass filtered (0.5–45 Hz) and then segmented in epochs ranging from −200 to +1344 ms from the first sound onset. We removed non-scalp EEG electrodes, leaving 195 electrodes in the next preprocessing steps. The EEG recordings were then preprocessed using the same fully automatic procedure as for the visual awareness paradigm and

the nap experiment. The remaining stimulus-locked epochs were averaged and digitally transformed to an average reference. A 200-ms baseline correction (before the fifth sound onset) was applied. In the LG dataset of the patient population, analyses were carried out from −100 ms before the onset of the first sound to the onset of the fifth sound (+600 ms), what we call above the "pseudo-resting-state." All trials are selected independently of standard or deviant status. Whereas for the healthy participants, we used the period between +600 ms, which is the onset of the fifth sound, and +1300 ms.

Computation of markers

Normalized power spectral analysis

Spectral analysis is a well-established method for the analysis of EEG signals. We estimated power in five frequency bands [delta to gamma: delta (δ: 1–4 Hz), theta (θ: 4–8 Hz), alpha (α: 8–13 Hz), beta (β: 13–30 Hz), and gamma (γ: 30–45 Hz)]. Mathematically, the power spectral density is estimated by the Welch method (Welch 1967). The power in a given band is calculated as the integral of the spectral power density then it is linearized using a logarithmic scale. The normalized power is calculated by dividing the power in each band by the total energy in the trial. It is expressed in dB and therefore represents a percentage of power. The abbreviations used in the text for the normalized power bands are the following: delta normalized $|\delta|$, theta normalized $|\theta|$, alpha normalized $|\alpha|$, beta normalized $|\beta|$, and gamma normalized $|\gamma|$.

Markers of complexity

"Permutation entropy (PE)" was developed by Bandt and Pompe (2002). The basic principle of this method is the transformation of the time signal into a sequence of symbols before estimating entropy. The complete description is given in Sitt et al. (2014). The transformation is made by considering consecutive subvectors of the signal of size n ($n = 3$ here) and a parameter defining a specific frequency band. After the symbolic transform, the probability of each symbol is estimated, and PE is computed by applying Shannon's entropy formula to the probability distribution of the symbols.

"The complexity of Kolmogorov–Chaitin (KS)" is represented by the size of the smallest computer program that can be made to define this signal. The lower limit is therefore estimated by applying lossless compression, that is to say, a compression that restores after decompression a series of bits strictly identical to the original. The degree of compression is then compared to the basic signal. Here we use an open-source compressor: gzip. It uses a compression algorithm, a method called Deflate including the LZ77 algorithm and Huffman coding.

The first is based on dictionary compression by transforming the sequence into 32 symbols, then we replace the recurring sequences with the position and the length of the occurrences in a sliding window. The second is based on constructing a tree where we assign a weight to each redundant sequence. Thus, after having calculated the number of occurrences of a sequence, the more redundant the sequence the more a small number of bits is allocated to code it. Compression by gzip is therefore based on signal redundancy. We then compare the size of the compression compared to the initial file. The more compressed the file, the less information it contains.

Markers of connectivity

The weighted symbolic mutual information (wSMI) can be used to evaluate long-distance connectivity, and details of the calculation are explained in King et al. (2013). The wSMI is a measure based on the prediction of the theory of the global workspace and experiments concerning the conscious perception of subliminal stimuli. Indeed, several studies (Dehaene et al. 2001, 2003) have shown a late use of the frontoparietal network and above all an increase in the sharing of information between brain areas. The EEG signal is transformed into a sequence of six symbolic figures then the PE)is calculated: we then take each pair of electrodes and observe the conjunction of symbolic elements. Mutual information measures the quantity of information distributed on average by a realization of X over the probabilities of realization of Y. The SMI is weighted to ignore conjunctions of identical or opposite symbols that may come from a common source of artifacts. The connectivity measurement is obtained by taking the median value of all pairs of electrodes.

Statistics

The area under the curve (AUC) is calculated from the ROC curve. The ROC curve is a graph representing the performance of a binary classification model for all classification thresholds. It is plotted from the rate of true positives (sensitivity) versus the rate of false positives (1 – specificity). It is then possible to calculate the area under this curve, or AUC, using a sorting algorithm. The AUC provides an aggregate measure of performance for all possible classification thresholds. The AUC can be interpreted as a measure of the probability that the EEG marker used will correctly classify trials or conditions (here, UWS/MCS patients, wake/N2 sleep in healthy participants, GD/GS, LD/LS; or seen/unseen trials). In our proposed framework, we use AUC to represent the performance of a given neuronal marker to distinguish two conditions (e.g. UWS versus MCS in the state dimension or seen versus unseen and different levels of cognitive processing in the content dimension) independent of a classifier—we only give the marker values and condition A or B. In our case conditions, condition A are seen, wake, LD, GD, and MCS, whereas condition B are unseen, sleep, LS, GS, and UWS. An AUC value close to 1 shows that the marker is higher in the A condition than in the B condition, close to 0.5 the distributions overlap, and an AUC value close to 0 shows that the marker is higher in the B condition than in the A condition. For the paired conditions (unseen/seen; sleep/wake; GS/GD; LS/LD), the distributions of the markers per epoch were z-scored, and the trimmed means were calculated (excluding the bottom and top 10% of the distributions). This results in one value per subject per condition per marker. The AUC values were calculated on these group-level distributions. For the UWS/MCS recordings, the same analysis was done with the exception of z-scoring. We report significant AUC for the content or the state if the AUC values of the two distributions are significantly different with a Wilcoxon two-sided test, Bonferroni corrected—for the paired conditions and a Mann–Whitney U test, Bonferroni corrected—for the unpaired condition (UWS/MCS).

The 2D framework: state versus content dimensions

We propose a system to study the state and content of consciousness in the same coordinate space. In our framework, we use the AUC to depict the performance of a specific neuronal marker, contrasting a binary classification of state (NM-S) along the x-axis (two examples provided: wake/sleep and UWS/MCS) and a binary classification of content (NM-C) along the y-axis (two examples: seen/unseen and GS/GD) (Fig. 1).

As an example of neuronal markers, we computed a set of previously proposed putative EEG markers (Sitt et al. 2014,

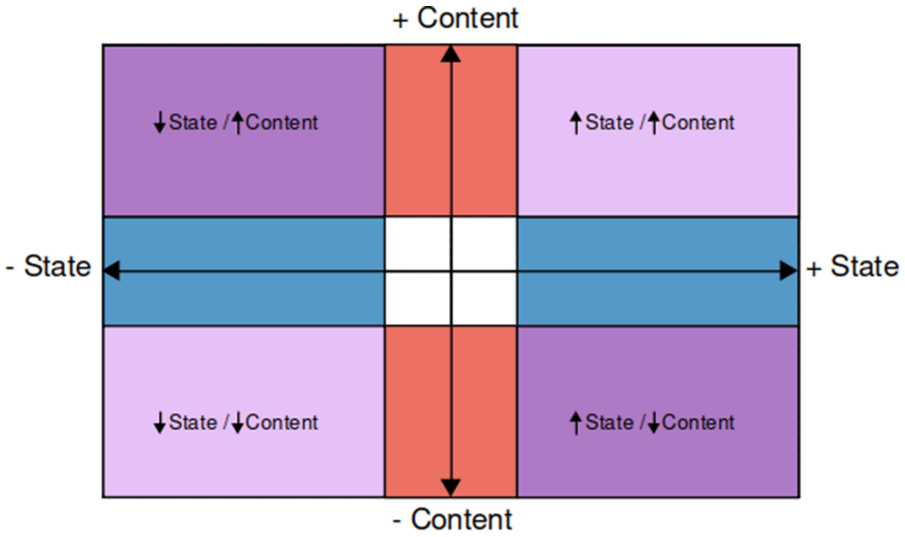

Figure 1 A 2D representation of state of consciousness and conscious content. The decomposition of the space forms four quadrants. The upper right and lower left quadrants correspond to the quadrants in which the content markers decrease when the level of consciousness decreases and vice versa; the upper left and lower right quadrants correspond to an increase of content markers when the level of consciousness decreases (or vice versa); the band around the x-axis represents a significant difference only in the state contrast, the band around the y-axis only for the content contrast, and the area around the origin is not specific to both content and state contrasts

Engemann et al. 2018) in state-of-consciousness contrasts and conscious content contrasts (either conscious access or contrasting two different levels of cognitive processing). The markers used in this study belong to a few conceptual families in neural dynamics (spectral, information theory, and connectivity) and are defined in the aforementioned studies (Sitt et al. 2014, Engemann et al. 2018) (also see the "Computation of markers" section). These markers have been shown to have discriminatory power across the DoC (Sitt et al. 2014, Engemann et al. 2018) and sleep spectra (Strauss et al. 2022, Türker et al. 2023). Importantly, the algorithms and parameters used to compute the proposed markers were identical in both cases.

Three types of markers were computed: (i) markers of connectivity—wSMI in the theta band (consciousness state sensitivity reported by King et al. 2013); (ii) markers of complexity—Kolmogorov–Chaitin complexity and PE; and (iii) markers of frequency power—delta power, theta power, alpha power, beta power, and gamma power. The result is expressed with the AUC quantifying each marker's discriminative power between the two groups within each contrast (e.g. wakefulness and N2 sleep or between MCS and UWS patients).

To test the implementation of the framework we provide a series of examples. In the first example, we used a popular contrast, the comparison of NM-Ss during wakefulness versus Stage 2 (N2) of NREM sleep in healthy participants. In the second example again for the conscious state (x-axis), we use the contrast between UWS patients and MCS patients, the UWS as a state of wakefulness without awareness and the MCS as an awake state with minimal or inconsistent awareness of self or the environment.

In our examples, conscious content (on the y-axis) is represented by the same markers used on the x-axis but in this case, contrasting a perceptual task between a conscious condition and an unconscious condition or contrasting two different levels of cognitive processing. We also use the AUC of each marker to differentiate between two conditions. We used two examples of conscious content tasks in healthy participants: (i) the visual awareness paradigm using a visual backward masking paradigm (contrasting seen/unseen trials and (ii) the auditory LG paradigm that is a complex auditory oddball paradigm (quantifying the marker differences between GD and GS trials, LD and LS trials).

The proposed axes divide the plane into four quadrants, subdivided into nine zones. The correspondence of each marker to a given quadrant determines how the marker behaves in terms of state and content (Fig. 1). The top right (AUC-x > 0.5 and AUC-y > 0.5) and bottom left (AUC-x < 0.5 and AUC-y < 0.5) quadrants in light violet correspond to markers that behave in unity in the state and content dimensions (increase in conscious state and conscious content or decrease in both dimensions). In contrast, the top left (AUC-x < 0.5 and AUC-y > 0.5) and bottom right (AUC-x > 0.5 and AUC-y < 0.5) quadrants in dark violet correspond to markers that have opposite behaviors in both dimensions (increase in conscious state and decrease conscious content, or vice versa). In addition, two blue/red zones around the x-/y-axis correspond to either an increase or decrease of the markers that are only valid for state (x, blue) or content (y, red), and the white area ~0.5 correspond to markers with no state- or content-specific information. The white zone in the middle of the plane represents markers unrelated to either state of content.

Results

Example 1: visual awareness paradigm and nap in healthy participants

In this example, we represent different EEG markers in the proposed 2D space to differentiate their behavior according to the state of consciousness or the conscious content (Fig. 2). For the x-axis, we use 26 EEG recordings in healthy participants during a nap opportunity of 2 h, and we order the markers according to the AUC discrimination on wakefulness versus N2 sleep. For the y-axis we used high-density EEG recordings in 35 healthy participants during a visual, backward masking, awareness paradigm (Del Cul et al. 2007). In this example, the values for each marker on the y-axis are determined by the AUC when contrasting seen versus unseen trials (Fig. 2).

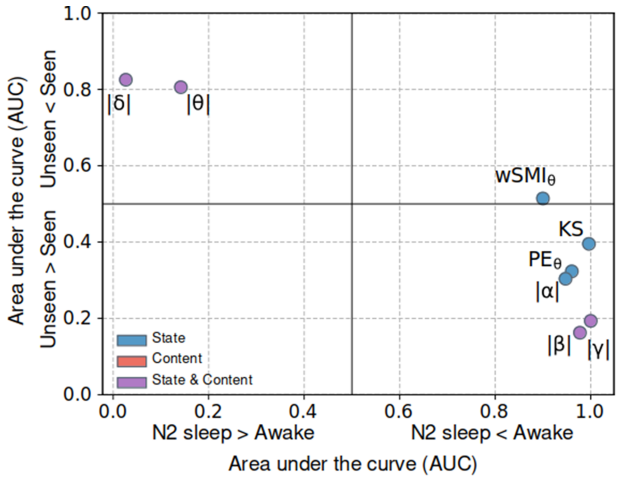

Figure 2 Example 1, behavior of EEG markers in the state and content dimensions for the visual awareness dataset and healthy participants nap. The coordinate of each point in the x-axis represents the ability of the marker to discriminate between wakefulness and N2 sleep; the coordinate in the y-axis of the same point represents the ability of the marker to discriminate between seen and unseen targets during the visual awareness paradigm; the values of the AUC and their confidence intervals, as well as the statistical test results, can be found in Supplementary Tables S1 and S2. KS: Kolmogorov complexity; wSMI: weighted mutual symbolic information; δ: delta; θ: theta, α: alpha; β: beta; γ: gamma

In the state dimension, described by the sleep and wake conditions, all markers had significantly different AUC values from 0.5 [Supplementary Tables S1 and S2; Fig. 2; $|\delta|$ (AUC = 0.026, $Z(2626) = 3$, $P < .0001$), $|\theta|$ (AUC = 0.142, $Z(2626) = 37$, $P = .01$), $|\alpha|$ (AUC = 0.947, $Z(2626) = 7$, $P < .0001$), $|\beta|$ (AUC = 0.977, $Z(2626) = 6$, $P < .0001$), $|\gamma|$ (AUC = 1, $Z(2626) = 0$, $P < .0001$), KS (AUC = 0.996, $Z(2626) = 1$, $P < .0001$), PE (AUC = 0.96, $Z(2626) = 8$, $P < .0001$), wSMI (AUC = 0.9, $Z(2626) = 23$, $P = .001$)]. Whereas in the content axis, represented by the experimental categories of seen and not seen visual stimuli, four of the markers are significantly different than 0.5 [$|\delta|$ (AUC = 0.825, $Z(3535) = 96$, $P = .001$), $|\theta|$ (AUC = 0.806, $Z(3535) = 122$, $P = .009$), $|\beta|$ (AUC = 0.162, $Z(3535) = 101$, $P = .002$), $|\gamma|$ (AUC = 0.193, $Z(3535) = 114$, $P = .005$)], which is not the case for the rest of the markers ($|\alpha|$ (AUC = 0.304, $Z(3535) = 169$, $P = .127$), KS (AUC = 0.395, $Z(3535) = 245$, $P = 1$), PE (AUC = 0.323, $Z(3535) = 186$, $P = .273$), wSMI (AUC = 0.514, $Z(3535) = 305$, $P = 1$)].

Most of the markers are on the lower right half of the graph ($|\alpha|$, $|\beta|$, $|\gamma|$, KS, wSMI, PE), but contrary to the second example, none of the markers are content-only. Interestingly, wSMI, KS, PE, and $|\alpha|$ are significant only for state, whereas $|\beta|$ and $|\gamma|$ are significant for both state and content. The two last markers $|\delta|$ and $|\theta|$ are in the top left quadrant and significant for both state and content, which means that they increase for content while they decrease with the state of consciousness.

Example 2: auditory LG paradigm and disorders of consciousness

For the second example, on the x-axis, representing level, we use the "pseudo resting state" (see the "Methods" section) of patients' data and we order the markers according to the AUC on the UWS versus MCS contrast. For the y-axis, representing content, we used the global–local paradigm in healthy participants' data and we sorted the markers according to the AUC on the GD versus GS conditions (Fig. 3a). Here we focus on the global contrast as it indicates some level of conscious content processing.

One part of the markers are significantly different than the threshold 0.5 for the state dimension contrasting UWS and MCS (Supplementary Tables S1 and S2; Fig. 3), specifically the markers $|\delta|$ [AUC = 0.38, $U(197\,191) = 14\,294$, $P = .0003$], $|\theta|$ [AUC = 0.649, $U(197\,191) = 24\,410$, $P < .0001$], $|\alpha|$ [AUC = 0.678, $U(197\,191) = 25\,520$, $P < .0001$], PE [AUC = 0.668, $U(197\,191) = 25\,138$, $P < .0001$], and wSMI [AUC = 0.656, $U(197\,191) = 24\,697$, $P < .0001$], which is not the case for the AUC values of $|\beta|$ [AUC = 0.528, $U(197\,191) = 19\,880$, $P = 1$], $|\gamma|$ [AUC = 0.481, $U(197\,191) = 18\,113$, $P = 1$] and KS [AUC = 0.559, $U(197\,191) = 21\,034$, $P = .355$]. Whereas all markers besides $|\theta|$ [AUC = 0.68, $Z(3636) = 208$, $P = .39$] had significant AUC values for the content dimension contrasting the conditions GS and GD {$|\delta|$ [AUC = 1, $Z(3636) = 0$, $P < .0001$], $|\alpha|$ [AUC = 0.033, $Z(3636) = 1$, $P < .0001$], $|\beta|$ [AUC = 0.077, $Z(3636) = 41$, $P < .0001$], $|\gamma|$ [AUC = 0.149, $Z(3636) = 80$, $P = .0002$], KS [AUC = 0.016, $Z(3636) = 3$, $P < .0001$], PE [AUC = 0.038, $Z(3636) = 8$, $P < .0001$], wSMI [AUC = 0.12, $Z(3636) = 13$, $P < .0001$]}.

Looking at the combined position in the coordinate system, the markers are arranged in all four quadrants (Fig. 3a). Several of the markers ($|\alpha|$, wSMI, PE, see the "Methods" section for the marker abbreviations) are located in the lower right quadrant, meaning that these markers increase with the state of consciousness but decrease with conscious content. Conversely, $|\delta|$ is on the upper left quadrant, indicating increasing values for conscious content but decreasing for the state of consciousness. Finally, other markers like $|\beta|$, $|\gamma|$, or KS were only significant for conscious content but not for state. Finally, $|\theta|$ was only significant for the conscious state but not for content, reflecting increasing values with the state of consciousness (minimally conscious > UWS states).

When looking into the LS/LD contrast, representing the content dimension (Supplementary Tables S1 and S2; Supplementary Fig. S1), all markers had significant AUC for the content dimension {$|\delta|$ [AUC = 0.857, $Z(3636) = 72$, $P < .0001$], $|\theta|$ [AUC = 0.764, $Z(3636) = 156$, $P = 0.037$], $|\alpha|$ [AUC = 0.188, $Z(3636) = 83$, $P = .0002$], $|\beta|$ [AUC = 0.243, $Z(3636) = 155$, $P = .035$], wSMI [AUC = 0.29, $Z(3636) = 134$, $P = .01$]}, except for $|\gamma|$ [AUC = 0.309, $Z(3636) = 194$, $P = .227$], KS [AUC = 0.355, $Z(3636) = 225$, $P = .732$], and PE [AUC = 0.322, $Z(3636) = 196$, $P = .246$].

Notably, a sharp difference in the AUC of the EEG markers can be observed when local or global contrasts are used for the content dimension (Fig. 3b; Supplementary Fig. S1). We present the differences between the two contrasts in terms of absolute value (–0.5) as we wish to show the amplitude or strength of the effect and not the directionality (here directionality refers to whether a given marker has a bigger value in LS compared to LD, or GS compared to GD). The performance of the markers to distinguish LD versus LS is systematically lower compared to GD versus GS (P-value .016 of a paired Wilcoxon signed-rank test). All but one ($|\theta|$) of the markers shows a lower discriminative performance for the global effect in contrast to the local effect.

Discussion

In this work, we propose a framework that permits the direct comparison of EEG markers of state and conscious content in the same space. With two implementation examples, we show that neural correlates depict different properties in discriminating these dimensions of consciousness.

The challenge in a 2D representation of neuronal markers of consciousness is to find a minimal relevant contrast. In these

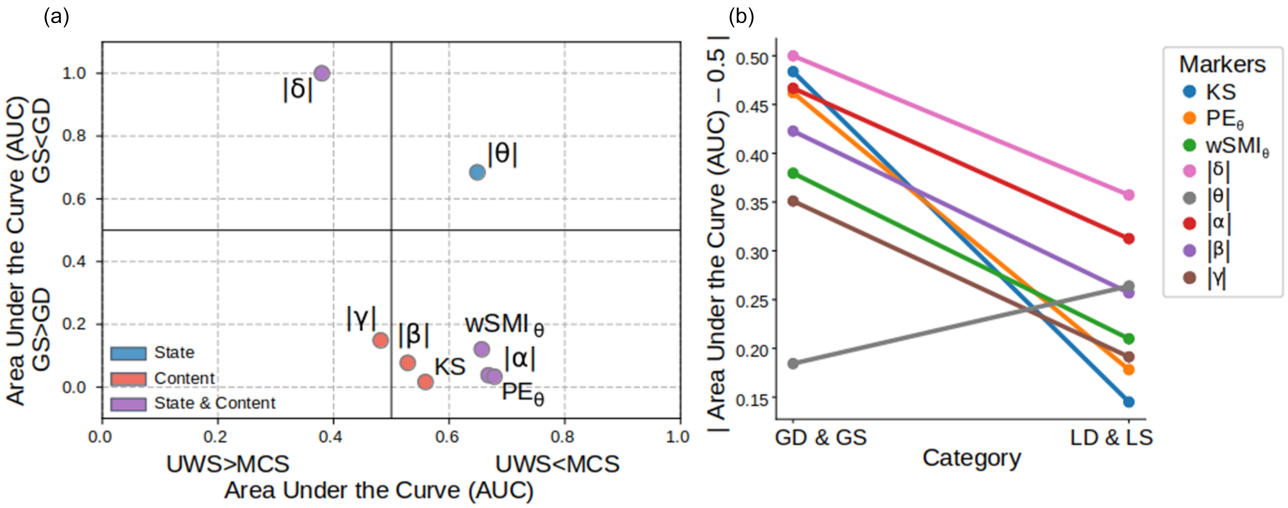

Figure 3 (a) Example 2, distribution of EEG markers in the state and content dimensions for the auditory modality and disorders of consciousness patients. The coordinate of each point in the *x*-axis represents the ability of the marker to discriminate between UWS and MCS patients. The coordinate at the same point in the *y*-axis represents the ability of the marker to discriminate between the GD and the GS trials in the LG paradigm in healthy participants. Note that the crossing of the *x*-axis and *y*-axis is centered at 0.5, which corresponds to discrimination at the level of chance. Points are colored according to their statistical significance in either the content dimension, the state dimension, or both. (b) The performance of EEG markers to discriminate GD to GS is higher than the power of EEG markers to discriminate LD to LS. The detection of the GD is a marker of conscious content, whereas the LD is an automatic response to the novelty. In the figure, 0.5 is subtracted from the values of the AUC. The values of the AUC and their confidence intervals, as well as the statistical test results, can be found in Supplementary Tables S1 and S2. KS: Kolmogorov complexity; wSMI: weighted mutual symbolic information; δ: delta; θ: theta, α: alpha; β: beta; γ: gamma

two examples, we contrast both conscious state and conscious content, but independently. The state was studied by contrasting healthy participants in non-REM Stage 2 sleep and in the awake state. We also studied the state condition by contrasting MCS patients and UWS patients, diagnosed in the clinic, since the MCS state is considered an altered state of consciousness, and the UWS state as a state of wakefulness without awareness. However, we have to note here that the UWS versus MCS contrast is less dichotomous than it seems due to the possibility that some UWS patients are in a covert conscious condition (as called cognitive motor dissociation) (Owen et al. 2006, Schiff 2015) as well as the heterogeneity within the two clinical categories (Naccache 2018, Hermann et al. 2021a). The conscious content was studied in two modalities: visual and auditory. There is a high distance in the contrast of the conscious content between the sensory modalities, but also due to the type of perceptual processing (masking, threshold vision, and detection of novelty), the challenge is to find a sufficiently salient contrast between the two conditions to capture, unambiguously, the perceptual or cognitive differences to obtain a robust neural characterization.

The first example, wake-sleep, and visual conscious access use the proposed representation with a task such as a visual perception protocol as well as other states of consciousness such as NREM sleep (Fig. 3). The second example, the auditory LG paradigm is particularly powerful because it allows for a dual analysis, first, the study of the early, automatic response to novelty (Fig. 3b; Supplementary Fig. S1), and, second, the late and conscious response (Fig. 3). The analysis of this early response is, therefore, a kind of control, since previous studies demonstrated that the brain processing of this rule does not require conscious awareness (Bekinschtein et al. 2009). In this example, we confirm with the LD/LS contrast that the putative EEG markers are less able to discriminate between the two conditions compared to the GD/GS contrast.

The comparison between the two examples highlights and challenges the fact that the different EEG markers evolve in the same direction according to the level of consciousness and the conscious content. One might intuitively hypothesize that most markers would be located in the light purple quadrants (top-right and bottom-left) of the graphical representation (Fig. 1), i.e. markers that increase with the state of consciousness and that also increase with the conscious content. In fact, most of the markers lie in the quadrants of the inverse relationship between state and content suggesting that they might play different roles in the state and content contrast. This result stresses the relevance of the proposed 2D framework to characterize simultaneously the behavior of markers in both the state and content dimensions.

Although the analyses of the exact location of each marker lie beyond the original objectives of this work, we will briefly interpret them. The NM-S analysis in the first example (Fig. 2) is mostly consistent with well-established knowledge of the relative spectral characteristics of wakefulness versus various sleep stages (Imperatori et al. 2021, Manasova and Stankovski 2023). In N2 sleep, we observe an increase in the relative delta and theta powers, as well as a decrease in alpha, beta, and gamma bands, which is aligned with previous reports (Imperatori et al. 2021) where all band comparisons are reported to be significant except for theta. Furthermore, we observe an increase in wSMI for the theta band in N2 sleep, which is present, but not strong enough (Imperatori et al. 2021). The NM-Ss in the second example (UWS/MCS contrast, Fig. 3) have an intuitive interpretation that is aligned with existing literature: while delta decreases with higher states of consciousness theta and alpha both increase and higher frequencies are less informative (Sitt et al. 2014).

In terms of conscious content in the first example (Fig. 2), we found that delta and theta were higher in seen conditions, and in the second example (Fig. 3) this is the case only for delta, which is higher in GD compared to the GS condition, that may reflect the

slow late potentials associated with conscious access, a process uniquely underlying awareness. In the first example (Fig. 2), contrary to some results in the literature we also found a reduction of gamma power, this is likely due to the more careful computation we used (20–40 Hz, the average across all electrodes, and normalized to the full spectrum power), as supported by Dwarakanath et al. (2023), who investigate the changes in conscious content in the prefrontal cortex using a binocular rivalry paradigm and show that there is a suppression of 20–40 Hz activity concurrent with 1–9 Hz transients, both of which follow the exogenous stimulus changes of physical stimulus alternations. Importantly, these high-frequency suppressions and 1–9 Hz transients precede the endogenous binocular rivalry perceptual transitions. The same is true for markers of complexity and functional connectivity that decrease in the post-perceptual period with conscious content (Example 1, Fig. 2). This could be explained by a "gating" mechanism, where the conscious perceptual input would close, creating a refractory period, which is reflected in a decrease of these markers in post-perceptual time. The reduction in complexity with conscious content is also compatible with the proposal of higher stability of neuronal activity during conscious access (Schurger et al. 2015).

Further reflecting on Figs 2 and 3 and the inverse relationship of the markers of content with those of the state, we can therefore think that there is a temporal constraint on the functional cognitive architecture theorized under the name of a cognitive cycle (Madl et al. 2011). According to its authors, awareness would consist of cascading cycles of recurrent cerebral events. Each cognitive cycle would then detect the current situation and interpret it according to a given context. According to Franklin et al. (2005), "conscious events occur as a sequence of discrete, coherent episodes separated by quite short periods of no conscious content" similar to the frames of a movie, and these frames of consciousness would be discrete but the conscious experience would seem continuous. A complementary framework is proposed by Herzog et al. (2016), where the authors argue for a rendering of the unconscious content in discrete conscious moments. They propose a two-stage model that is different from "snapshot" theories. Visual information is processed unconsciously with a high temporal resolution followed by a discrete conscious percept (the outputs of unconscious processing) at a slower rate than the visual sampling (Herzog et al. 2016). This rate of conscious percepts is not fixed but depends on the unconscious processing reaching an attractor state (Herzog et al. 2016).

Advantages, limitations, and opportunities of the proposed framework

The proposed framework is flexible and can be extended to, for example, subcategories of states of consciousness such as MCS+ versus MCS– but also to choose contrasts in other circumstances: rapid eye movement sleep, lucid dreams or anesthesia in healthy participants. Although these contrasts have not been presented here, as long as there is a grounded rationale of a given contrast (e.g. the difference of language comprehension and the underlying metabolic network activations in MCS– and MCS+ patients), this framework can be applied. This framework is also generalizable across functional modalities and markers. Here we use EEG recordings that have a high temporal resolution and can capture fast neural changes in response to the aforementioned task paradigms. But this framework can be extended to other neuroimaging modalities that allow distinction of state and content of consciousness (e.g. functional magnetic resonance, magnetoencephalography, intracranial recordings, fNIRS, and calcium imaging).

The two examples presented here should only be considered use cases, and we postulate that the proposed space characterizing neuronal markers of consciousness should be compatible with types of contrasts represented in the *y*-axis (e.g. crowding protocols, subliminal images, binocular rivalry, and non-report paradigms) or in the *x*-axis (e.g. anesthesia, epileptic seizures, and developmental stages). In a similar vein, the markers that we used to populate the coordinate space are examples of EEG-based markers used in the literature, our proposed framework permits to include any markers (and in any neuroimaging modality) as long as it can be computed in state and content assessments.

We would like to emphasize that although we map the space of these content and level correlates, we do not imply that only empirical neuronal markers (and not their underlying mechanisms) can be studied. Ideas coming from information theory such as the information decomposition approach (Mediano et al. 2022, Vinck et al. 2023) and biophysical models (Luppi et al. 2023) try to capture the neural signatures that are potential echoes (and not correlates) of the neural implementation of the processing of a content or the underlying dynamics that maintain a specific state. The framework that we propose can in turn be used as one form of evaluation of these models. For example, summary metrics of a biophysical model, or neural signatures that can be interpreted in terms of information and not simple communication or shared oscillatory activity, can be put into the 2D space and depending on whether they underlie processes of states of consciousness or process of the perception of specific contents, they will be expected in a certain quadrant.

Conclusion

Our study introduces a novel 2D state–content space that effectively represents EEG markers related to the state and content of consciousness. This innovative framework reveals significant relationships between these markers across both dimensions. In our examples, we observed an anticorrelation between the state and content dimensions in certain EEG markers, indicating that as one dimension's value increases, the other's decreases. This finding highlights the nuanced interplay between state and content markers and provides deeper insights into their behavior. The proposed 2D space has broad applicability across different perceptual modalities and various contrasts, offering a unified framework for examining consciousness. The value of this representation is both theoretical and experimental because it allows to disentangle content and state of consciousness signatures by studying multiple contrasts in the same framework, constituting an important tool to better interpret the true neuronal mechanisms underlying consciousness and cognition in different states and for different contents.

Acknowledgements

We would like to thank Mathias Michel for their help with the conceptualization of the study and for feedback on the manuscript. We thank all of the participants who took part in the studies. We would like to thank the work and support of the clinicians at the Neuro ICU, DMU Neurosciences, APHP-Sorbonne Université, Hôpital de la Pitié Salpêtrière, Paris, France, and the patient families whose consent and understanding are essential to the progress of the field.

Author contributions

Pauline Perez (Conceptualization, Methodology, Software, Formal analysis, Investigation, Data curation, writing—original draft, Visualization), Dragana Manasova (Methodology, Software, Formal analysis, Data curation, Writing—original draft, Writing—review & editing, Visualization), Bertrand Hermann (Investigation, Writing—review & editing), Federico Raimondo (Software, Writing—review & editing), Benjamin Rohaut (Investigation), Tristán A. Bekinschtein (Writing—review & editing, Funding acquisition), Lionel Naccache (Writing—review & editing, Funding acquisition), Anat Arzi (Investigation, Writing—review & editing, Visualization, Supervision), and Jacobo D. Sitt (Conceptualization, Methodology, Writing—review & editing, Supervision, Project administration, Funding acquisition).

Supplementary data

Supplementary data is available at *Neuroscience of Consciousness* online.

Conflict of interest

Jacobo D. Sitt and Lionel Naccache are scientific co-founders of NeuroMeters (have scientific advisory activity but no executive or management activity).

Funding

This work was supported by the Ecole Doctorale Frontières de l'Innovation en Recherche et Education–Programme Bettencourt (to D.M.), by Sorbonne Université (to P.P.), and by a Marie Curie Individual Fellowship (840711 awarded to A.A.). This project is part of the multicentric application for the EU ERAPerMed Joint Translational Call for Proposals for "Personalised Medicine: Multidisciplinary research towards implementation" (ERA PerMed JTC2019). It is funded by local funding agencies of the participating countries (for France it is the Agence Nationale de Recherche ANR, funding code: ANR-19-PERM-0002). This project is supported by the Human Brain Project (HBP) MODELDxConsciousness Consortium (Agence Nationale de Recherche ANR, funding code: S.1600.ANR.HBPR). Preliminary ideas of this work were presented in the NCC Symposium on the 23th ASSC Meeting (London, ON, 2019).

Data availability

The data used in this study can be made available upon reasonable request. Because of the sensitive nature of the clinical information concerning the patients, the ethics protocol does not allow open data sharing. To access the raw data, the potential interested researcher would need to contact the corresponding authors of the study. Together they would need to ask for an authorization from the local ethics committee, CPP Île de France 1 (Paris, France).

References

Andrillon T. How we sleep: from brain states to processes. *Rev Neurol (Paris)* 2023;**179**:649–57.

Andrillon T, Burns A, Mackay T *et al.* Predicting lapses of attention with sleep-like slow waves. *Nat Commun* 2021;**12**:3657.

Andrillon T, Kouider S. The vigilant sleeper: neural mechanisms of sensory (de)coupling during sleep. *Curr Opin Physiol* 2020;**15**:47–59.

Andrillon T, Oudiette D. What is sleep exactly? Global and local modulations of sleep oscillations all around the clock. *Neurosci Biobehav Rev* 2023;**155**:105465.

Bachmann T. How to begin to overcome the ambiguity present in differentiation between contents and levels of consciousness? *Front Psychol* 2012;**3**:1–6.

Bandt C, Pompe B. Permutation entropy: a natural complexity measure for time series. *Phys Rev Lett* 2002;**88**:174102.

Barttfeld P, Uhrig L, Sitt JD *et al.* Signature of consciousness in the dynamics of resting-state brain activity. *Proc Natl Acad Sci USA* 2015;**112**:887–92.

Bayne T, Hohwy J, Owen AM. Are there levels of consciousness? *Trends Cognit Sci* 2016;**20**:405–13.

Bekinschtein TA, Dehaene S, Rohaut B *et al.* Neural signature of the conscious processing of auditory regularities. *Proc Natl Acad Sci USA* 2009;**106**:1672–7.

Berry RB, Brooks R, Gamaldo CE *et al.* The AASM manual for the scoring of sleep and associated events. Rules Terminol Technical Specifications, Darien, Illinois. *Am Acad Sleep Med* 2012;**176**:7.

Blumenfeld H. Arousal and consciousness in focal seizures. *Epilepsy Curr* 2021;**21**:353–9.

Boly M, Seth AK, Wilke M *et al.* Consciousness in humans and non-human animals: recent advances and future directions. *Front Psychol* 2013;**4**:625.

Bruno MA, Vanhaudenhuyse A, Thibaut A *et al.* From unresponsive wakefulness to minimally conscious PLUS and functional locked-in syndromes: recent advances in our understanding of disorders of consciousness. *J Neurol* 2011;**258**:1373–84.

Casarotto S, Comanducci A, Rosanova M *et al.* Stratification of unresponsive patients by an independently validated index of brain complexity. *Ann Neurol* 2016;**80**:718–29.

Chalmers D. Moving forward on the problem of consciousness. *J Conscious Stud* 1997;**4**:3–46.

Chennu S, Finoia P, Kamau E *et al.* Spectral signatures of reorganised brain networks in disorders of consciousness. *PLoS Comput Biol* 2014;**10**: e1003887.

Chennu S, Noreika V, Gueorguiev D *et al.* Expectation and attention in hierarchical auditory prediction. *J Neurosci* 2013;**33**: 11194–205.

Chennu S, O'Connor S, Adapa R *et al.* Brain connectivity dissociates responsiveness from drug exposure during propofol-induced transitions of consciousness. *PLoS Comput Biol* 2016;**12**: e1004669.

Comsa IM, Bekinschtein TA, Chennu S. Transient topographical dynamics of the electroencephalogram predict brain connectivity and behavioural responsiveness during drowsiness. *Brain Topogr* 2019;**32**:315–31.

Crick F, Koch C. Towards a neurobiological theory of consciousness. *Sem Neurosci* 1990;**2**:263–75.

Dang-Vu TT, Schabus M, Desseilles M *et al.* Functional neuroimaging insights into the physiology of human sleep. *Sleep* 2010;**33**:1589–603.

Dehaene S, Changeux JP. Experimental and theoretical approaches to conscious processing. *Neuron* 2011;**70**:200–27.

Dehaene S, Naccache L, Cohen L *et al.* Cerebral mechanisms of word masking and unconscious repetition priming. *Nat Neurosci* 2001;**4**:752–8.

Dehaene S, Sergent C, Changeux J-P. A neuronal network model linking subjective reports and objective physiological data during conscious perception. *Proc Natl Acad Sci USA* 2003;**100**:8520–5.

Del Cul A, Baillet S, Dehaene S. Brain dynamics underlying the nonlinear threshold for access to consciousness. *PLoS Biol* 2007;**5**:2408–23.

Demertzi A, Antonopoulos G, Heine L *et al.* Intrinsic functional connectivity differentiates minimally conscious from unresponsive patients. *Brain* 2015;**138**:2619–31.

Demertzi A, Gómez F, Crone JS *et al*. Multiple fMRI system-level baseline connectivity is disrupted in patients with consciousness alterations. *Cortex J Devoted Study Nerv Syst Behav* 2014;**52**:35–46.

Demertzi A, Tagliazucchi E, Dehaene S *et al*. Human consciousness is supported by dynamic complex patterns of brain signal coordination. *Sci Adv* 2019;**5**:eaat7603.

Di Perri C, Bahri MA, Amico E *et al*. Neural correlates of consciousness in patients who have emerged from a minimally conscious state: a cross-sectional multimodal imaging study. *Lancet Neurol* 2016;**15**:830–42.

Dwarakanath A, Kapoor V, Werner J *et al*. Bistability of prefrontal states gates access to consciousness. *Neuron* 2023;**111**:1666–83.e4.

Edlow BL, Claassen J, Schiff ND *et al*. Recovery from disorders of consciousness: mechanisms, prognosis and emerging therapies. *Nat Rev Neurol* 2021;**17**:135–56.

Engemann DA, Raimondo F, King JR *et al*. Robust EEG-based cross-site and cross-protocol classification of states of consciousness. *Brain* 2018;**141**:3179–92.

Franklin S, Baars BJ, Ramamurthy U *et al*. The role of consciousness in memory. *Brains Minds Media*2005;**1**:4.

Giacino JT, Ashwal S, Childs N *et al*. The minimally conscious state: definition and diagnostic criteria. *Neurology* 2002;**58**: 349–53.

Goupil L, Bekinschtein TA. Cognitive processing during the transition to sleep. *Arch Ital Biol* 2012;**150**:140–54.

Guo JN, Kim R, Chen Y *et al*. Mechanism of impaired consciousness in absence seizures: a cross-sectional study. *Lancet Neurol* 2016;**15**:1336–45.

Hermann B, Sangaré A, Munoz-Musat E *et al*. Importance, limits and caveats of the use of "disorders of consciousness" to theorize consciousness. *Neurosci Conscious* 2021a;**2021**:1–13.

Hermann B, Stender J, Habert MO *et al*. Multimodal FDG-PET and EEG assessment improves diagnosis and prognostication of disorders of consciousness. *NeuroImage Clin* 2021b;**30**:102601.

Herzog MH, Kammer T, Scharnowski F. Time slices: what is the duration of a percept? *PLOS Biol* 2016;**14**:e1002433.

Imperatori LS, Cataldi J, Betta M *et al*. Cross-participant prediction of vigilance stages through the combined use of wPLI and wSMI EEG functional connectivity metrics. *Sleep* 2021;**44**:zsaa247.

Jennett B, Plum F. Persistent vegetative state after brain damage: a syndrome in search of a name. *Lancet* 1972;**299**:734–7.

Kalmar K, Giacino J. The JFK coma recovery scale—revised. *Neuropsychol Rehabil* 2005;**15**:454–60.

Kim C-Y, Blake R. Psychophysical magic: rendering the visible "invisible". *Trends Cognit Sci* 2005;**9**:381–8.

King JR, Sitt JD, Faugeras F *et al*. Information sharing in the brain indexes consciousness in noncommunicative patients. *Curr Biol* 2013;**23**:1914–9.

Koch C, Massimini M, Boly M *et al*. Neural correlates of consciousness: progress and problems. *Nat Rev Neurosci* 2016;**17**:307–21.

Laureys S, Celesia GG, Cohadon F *et al*. Unresponsive wakefulness syndrome: a new name for the vegetative state or apallic syndrome. *BMC Med* 2010;**8**:68.

Laureys S, Owen AM, Schiff ND. Brain function in coma, vegetative state, and related disorders. *Lancet Neurol* 2004;**3**:537–46.

Leslie K, Skrzypek H, Paech MJ *et al*. Dreaming during anesthesia and anesthetic depth in elective surgery patients: a prospective cohort study. *Anesthesiology* 2007;**106**:33–42.

Lewis LD, Weiner VS, Mukamel EA *et al*. Rapid fragmentation of neuronal networks at the onset of propofol-induced unconsciousness. *Proc Natl Acad Sci USA* 2012;**109**:19891.

Luppi AI, Cabral J, Cofre R *et al*. Computational modelling in disorders of consciousness: closing the gap towards personalised models for restoring consciousness. *NeuroImage* 2023;**275**:120162.

Madl T, Baars BJ, Franklin S. The timing of the cognitive cycle. *PLoS ONE* 2011;**6**:e14803.

Manasova D, Stankovski T. Neural cross-frequency coupling functions in sleep. *Neuroscience* 2023;**523**:20–30.

Mediano PAM, Rosas FE, Luppi AI *et al*. Greater than the parts: a review of the information decomposition approach to causal emergence. *Philos Trans R Soc A* 2022;**380**.

Naccache L. Minimally conscious state or cortically mediated state? *Brain* 2018;**141**:949–60.

Owen AM, Coleman MR, Boly M *et al*. Detecting awareness in the vegetative state. *Science* 2006;**313**:1402.

Peigneux P. Neuroimaging studies of sleep and memory in humans. *Curr Top Behav Neurosci* 2014;**25**:239–68.

Perrin F, Pernier J, Bertrand O *et al*. Spherical splines for scalp potential and current density mapping. *Electroencephalogr Clin Neurophysiol* 1989;**72**:184–7.

Sanders RD, Tononi G, Laureys S *et al*. Unresponsiveness ≠ unconsciousness. *Anesthesiology* 2012;**116**:946–59.

Schiff ND. Cognitive motor dissociation following severe brain injuries. *JAMA Neurol* 2015;**72**:1413–5.

Schurger A, Sarigiannidis I, Naccache L *et al*. Cortical activity is more stable when sensory stimuli are consciously perceived. *Proc Natl Acad Sci USA* 2015;**112**:E2083–92.

Sergent C, Corazzol M, Labouret G *et al*. Bifurcation in brain dynamics reveals a signature of conscious processing independent of report. *Nat Commun* 2021;**12**:1–19.

Sergent C, Faugeras F, Rohaut B *et al*. Multidimensional cognitive evaluation of patients with disorders of consciousness using EEG: a proof of concept study. *NeuroImage Clin* 2017;**13**:455–69.

Sitt JD, King JR, El Karoui I *et al*. Large scale screening of neural signatures of consciousness in patients in a vegetative or minimally conscious state. *Brain* 2014;**137**:2258–70.

Solms M. Dreaming and REM sleep are controlled by different brain mechanisms. *Behav Brain Sci* 2000;**23**:843–50.

Song C, Tagliazucchi E. Linking the nature and functions of sleep: insights from multimodal imaging of the sleeping brain. *Curr Opin Physiol* 2020;**15**:29–36.

Stender J, Gosseries O, Bruno M-A *et al*. Diagnostic precision of PET imaging and functional MRI in disorders of consciousness: a clinical validation study. *Lancet* 2014;**384**:514–22.

Strauss M, Sitt JD, King JR *et al*. Disruption of hierarchical predictive coding during sleep. *Proc Natl Acad Sci USA* 2015;**112**: E1353–62.

Strauss M, Sitt JD, Naccache L *et al*. Predicting the loss of responsiveness when falling asleep in humans. *NeuroImage* 2022;**251**: 119003.

Tsuchiya N, Wilke M, Frässle S *et al*. No-report paradigms: extracting the true neural correlates of consciousness. *Trends Cognit Sci* 2015;**19**:757–70.

Türker B, Musat EM, Chabani E *et al*. Behavioral and brain responses to verbal stimuli reveal transient periods of cognitive integration of the external world during sleep. *Nat Neurosci* 2023;**26**:1–13.

Vinck M, Uran C, Spyropoulos G *et al*. Principles of large-scale neural interactions. *Neuron* 2023;**111**:987–1002.

Wacongne C, Labyt E, van Wassenhove V *et al*. Evidence for a hierarchy of predictions and prediction errors in human cortex. *Proc Natl Acad Sci USA* 2011;**108**:20754–9.

Welch P. The use of fast Fourier transform for the estimation of power spectra: a method based on time averaging over short, modified periodograms. *IEEE Trans Audio Electroacoustics* 1967;**15**: 70–3.

Zelmann R, Paulk AC, Tian F *et al*. Differential cortical network engagement during states of un/consciousness in humans. *Neuron* 2023;**111**:3479–95.e6.

Neuroscience of Consciousness, 2024, 2024(1), niae027 , DOI: https://doi.org/10.1093/nc/niae027, Research Article
Received 8 November 2023; revised 30 May 2024; accepted 8 June 2024